Mathematical Modelling and Numerical Simulation with Applications, 2024, 4(3), 256–279

https://dergipark.org.tr/en/pub/mmnsa

ISSN Online: 2791-8564 / Open Access

https://doi.org/10.53391/mmnsa.1484994

RESEARCH PAPER

A three-dimensional discrete fractional-order HIV-1 model related to cancer cells, dynamical analysis and chaos control

Haneche Nabil [1,*,‡] and **Hamaizia Tayeb** [2,‡]

[1]Applied Mathematics & Modeling Laboratory, Department of Mathematics, University of Mentouri Brothers, 25000 Constantine, Algeria, [2]Department of Mathematics, University of Mentouri Brothers, 25000 Constantine, Algeria

* Corresponding Author

‡ nabil.haneche@doc.umc.edu.dz (Haneche Nabil); el.tayyeb@umc.edu.dz (Hamaizia Tayeb)

Abstract

In this paper, we study a three-dimensional discrete-time model to describe the behavior of cancer cells in the presence of healthy cells and HIV-infected cells. Based on the Caputo-like difference operator, we construct the fractional-order biological system. This study's significance lies in developing a new approach to presenting a biological dynamical system. Since the qualitative analysis related to existence, uniqueness, and stability is almost the same as can be found in numerous existing papers, and comparing this study to other research, constructing a biological discrete system using the Caputo difference operator can be particularly important. Using powerful tools of nonlinear theory such as phase plots, bifurcation diagrams, Lyapunov exponent spectrum, and the 0-1 test, we establish that the proposed system can exhibit different biological states, including stable, periodic, and chaotic behaviors. Here, the route leading to chaos is period-doubling bifurcation. Furthermore, the level of chaos in the system is quantified using C_0 complexity and approximate entropy algorithms. The stabilization or suppression of chaotic motions in the fractional-order system is presented, where an efficient controller is designed based on the stability theory of the discrete-time fractional-order systems. Numerical simulations are provided to validate the theoretical results derived in this research paper.

Keywords: Fractional-order; discrete chaos; HIV-1 model; bifurcation diagram; chaos control

AMS 2020 Classification: 26A33; 34H10; 35B41; 37D45; 37G35

1 Introduction

In recent years, the modeling of infectious diseases has become an important topic that has been studied to describe the mechanisms by which disease spreads and then to predict the future behavior of the disease. The goal of this study is to find solutions and strategies to fight and

➤ **Received:** 16.05.2024 ➤ **Revised:** 06.07.2024 ➤ **Accepted:** 15.07.2024 ➤ **Published:** 30.09.2024

control epidemics and diseases such as cancers and immunodeficiency disease [1]. Mathematical systems can be used to design new experiments by formulating hypotheses about the spread and dynamics of disease. In particular, nowadays, mathematical models of HIV-1 have been extensively studied by researchers around the world to show the interactions between healthy cells, infected cells, and cancer cells. There are many existing reviews of HIV-1 models that describe the coexistence of HIV-infected cells with cancer cells, see [2–5]. Our contribution is to construct a discrete fractional-order model that describes the interactions between these cells, and then to control the constructed system via an effective fractional-order controller.

Recently, discrete-time systems have been more commonly used than continuous-time systems to study biological and epidemiological models because discrete-time systems are easier to compute and numerically simulate [6]. In fact, fractional calculus is a broad field in modern mathematics that allows us to investigate and describe a new phenomenon modeled with fractional-order equations. To our best knowledge, the first idea of the fractional derivative is associated with Leibniz when he discussed the possibility of the construction of a fractional derivative in correspondence with Bernoulli and Wallis in 1695 [7]. Then, the complete definition of such fractional derivative was not established until the 19^{th} century as a result of the works of Letnikov, Grunwald, Liouville, Riemann, etc [8]. It should be noted that Letnikov established the first exact theoretical formulation of the fractional derivation. Today, many types of fractional derivatives exist, with and without singular kernels. With singular kernels, we have the well-known fractional derivatives, Caputo fractional derivative [9] and Riemann-Liouville fractional derivative [10]. Without singular kernels, we have two categories: fractional derivative with the exponential kernel which is the Caputo-Fabrizio fractional derivative [11], and fractional derivative with Mittag-Leffler kernel which is called as Atangana-Baleanu fractional derivative [12].

Modeling biological systems with fractional derivatives becomes an important topic due to the involvement of memory and hereditary properties in the study of the interaction between cancer cells and HIV-infected cells [13]. The non-integer models incorporate all prior information from the past due to the memory effect, then we can understand well the dynamics of the model and predict the spread of the disease [14]. The topics of stability of the equilibrium points, existence and uniqueness, positivity and boundedness of the solution in the fractional order cancer models are discussed in detail in [15–20]. Several numerical solutions to solve fractional-order biological systems are proposed in [21–23].

Nowadays, among several fractional derivatives that exist, the Riemann-Liouville derivative and the Caputo derivative are the most commonly used [24]. Today, many systems in physics, chemistry, biology, epidemiology, neurology, viscoelasticity, cryptography, cardiology, etc. have been studied and developed using fractional calculus theory [25].

On the side of discrete dynamical systems, Diaz and Osler published in 1974 the first concept of a fractional difference operator defined as a generalization of the binomial formula for the n^{th}-order difference operator Δ^n [26]. Furthermore, Atici et al. introduced the fractional nabla difference operator, which is analogous to the forward fractional difference proposed by Miller and Ross in 1989 [27]. Then, Abdeljawad introduced the Caputo fractional delta and nabla difference operators [28]. Recently, Abdeljawad et al. derived the delta and nabla discrete formulas for fractional integral and derivative, adopting the binomial theorem [29].

Discrete fractional calculus allows us to study systems in biology and ecology using fractional-order equations to get better results and understand the interactions between species. Another advantage of this theory is the speed of calculations with high precision. Additionally, it consumes minimal computer resources [30]. While discrete fractional calculus offers benefits such as high flexibility and robustness, it also poses challenges related to nonlinearity and complexity when we numerically solve a fractional-order system. Furthermore, this theory's analytical tools have

limitations in determining the convergence and stability of numerical schemes. Using numerical methods and approximations to solve a fractional-order equation can lead to significant errors [31].

Recently, there has been great interest shown in the literature on chaotic dynamical systems due to their important applications in practice. A chaotic system is defined as a dynamical system that displays what is called sensitive dependence on initial conditions [32]. A small change in the initial state of a chaotic system may lead to completely different outcomes. In nonlinear dynamical analysis, a chaotic system has at least one positive Lyapunov exponent, in which the Lyapunov exponent is a numerical quantity that measures the rate of convergence and divergence of neighboring trajectories in nonlinear dynamical system [33].

In the current paper, we report a 3-D discrete-time fractional-order HIV-1 model involving AIDS-related cancer cells. This model can exhibit chaotic dynamics for some parameter values. By employing theoretical results and numerical simulations, we can show the chaotic behavior of the proposed system, which is a popular phenomenon in nonlinear dynamical systems. In Section 2, basic notions related to discrete fractional calculus are introduced. In Section 3, the discrete fractional-order system is constructed based on the Caputo-like delta difference operator. In Section 4, the dynamics of the fractional-order system are analyzed in both commensurate and non-commensurate fractional-order using powerful tools in nonlinear dynamic analysis such as phase portraits, bifurcation diagrams, maximum Lyapunov exponent, dynamical maps, etc. In Section 5, the complexity of the fractional-order system is measured by the 0-1 test, C_0 complexity, and approximate entropy algorithms. In Section 6, a suitable control scheme for stabilizing the chaotic dynamics in the fractional-order system is constructed. In Section 7, the data analysis and discussion have been presented. Section 8 contains the conclusions.

2 Mathematical background

In this section, we give some results of discrete fractional calculus, which helped us build this manuscript.

Definition 1 *[27] Consider the real-valued function $\phi(\tau) : \mathbb{N}_\alpha \to \mathbb{R}$ with $\mathbb{N}_\alpha = \mathbb{N}_0 + \{\alpha\} = \{\alpha, \alpha+1, \alpha+2, \ldots\}$ where $\alpha \in \mathbb{R}$. Let $\nu > 0$, the ν^{th}-order fractional sum of $\phi(\tau)$ is defined as*

$$\Delta_\alpha^{-\nu}\phi(\tau) = \frac{1}{\Gamma(\nu)}\sum_{\xi=\alpha}^{\tau-\nu}(\tau-\xi-1)^{(\nu-1)}\phi(\xi), \tag{1}$$

where the falling factorial $\tau^{(\nu)}$ is expressed using the Γ-function as

$$\tau^{(\nu)} = \frac{\Gamma(\tau+1)}{\Gamma(\tau+1-\nu)} = \tau\,(\tau-1)\ldots(\tau-\nu+1)\,. \tag{2}$$

Definition 2 *[28] Let $\phi(\tau) : \mathbb{N}_{\alpha+(m-\nu)} \to \mathbb{R}$ a real-valued function and $\nu \notin \mathbb{N}$, the Caputo-like discrete fractional difference operator of $\phi(\tau)$ is defined as*

$${}^{C}\Delta_\alpha^{\nu}\phi(\tau) = \Delta_\alpha^{-(m-\nu)}\Delta^m\phi(\tau) = \frac{1}{\Gamma(m-\nu)}\sum_{\xi=\alpha}^{\tau-(m-\nu)}(\tau-\xi-1)^{(m-\nu-1)}\Delta_\xi^m\phi(\xi), \tag{3}$$

where $\nu \notin \mathbb{N}$, $m = [\nu]+1$ and $\tau \in \mathbb{N}_{\alpha+(m-\nu)}$.

By adopting the following theorem, we can define the numerical solution of a discrete fractional-

order system.

Theorem 1 *[34] Given the following Caputo-type discrete initial value problem*

$$\begin{cases} {}^{C}\Delta_{\alpha}^{\nu}\phi(\tau) = \psi(\tau+\nu-1,\phi(\tau+\nu-1)), \\ \Delta^{k}\phi(\alpha) = \phi_{k}, \quad m=[\nu]+1, \quad k=0,1,2,\ldots,m-1, \end{cases} \tag{4}$$

then the unique solution of problem (4) is given by

$$\phi(\tau) = \phi_{0}(\tau) + \frac{1}{\Gamma(\nu)} \sum_{\xi=\alpha+(m-\nu)}^{\tau-\nu} (\tau-\xi-1)^{(\nu-1)}\psi(\xi+\nu-1,\phi(\xi+\nu-1)), \quad \tau \in \mathbb{N}_{\alpha+m}, \tag{5}$$

where

$$\phi_{0}(\tau) = \sum_{k=0}^{m-1} \frac{(\tau-\alpha)^{(k)}}{\Gamma(k+1)}\Delta^{k}\phi(\alpha) = \sum_{k=0}^{m-1} \frac{(\tau-\alpha)^{(k)}}{k!}\Delta^{k}\phi(\alpha). \tag{6}$$

The next theorem allows us to construct a stability condition for an equilibrium point of a discrete fractional-order system in the case of commensurate fractional order.

Theorem 2 *[35] For the discrete commensurate fractional-order system*

$${}^{C}\Delta_{\alpha}^{\nu}S(\tau) = BW(\tau+\nu-1), \tag{7}$$

where $W(\tau) = (w_{1}(\tau), w_{2}(\tau), \ldots, w_{n}(\tau))^{T}$, $B \in \mathbb{R}^{n\times n}$, *and* $\tau \in \mathbb{N}_{(\alpha-\nu)+1}$, *the zero equilibrium point of (7) is asymptotically stable if*

$$\lambda_{j} \in \left\{ z_{0} \in \mathbb{C} : |z_{0}| < \left(2\cos\frac{|\arg z_{0}|-\pi}{2-\nu}\right)^{\nu} \quad \text{and} \quad |\arg z_{0}| > \nu\frac{\pi}{2} \right\}, \qquad j=1,2,\ldots,n, \tag{8}$$

where λ_{j} *is an eigenvalue of the matrix* B *and* $\nu \in (0,1)$.

3 Discrete fractional-order HIV-1 model

Recently, Lou et al. [36] proposed a three-dimensional continuous-time HIV-1 system with cancer cells related to AIDS, which is described by the following dynamics:

$$\begin{cases} \frac{dC}{dt} = C\left[\alpha_{1}\left(1-\frac{C+S+R}{\mu}\right)-\delta_{1}S\right], \\ \frac{dS}{dt} = S\left[\alpha_{2}\left(1-\frac{C+S+R}{\mu}\right)-\eta\delta_{1}C-\delta_{2}R\right], \\ \frac{dR}{dt} = R\left(\delta_{2}S-\varrho\right), \end{cases} \tag{9}$$

where C represents the number of cancer cells, S represents the number of healthy cells, and R represents the number of HIV-infected cells. α_{1}, α_{2}, μ, δ_{1}, δ_{2}, η, and ϱ are constant positive parameters. Here α_{1} and α_{2} represent the rate at which cancer cells proliferate uncontrollably and the healthy cells' inherent growth rate respectively, with always $\alpha_{1} > \alpha_{2}$, then the cancer cells reproduce faster than the healthy cells. δ_{1} represents the immune system's capacity to eliminate cancerous cells, δ_{2} represents the rate coefficient of infection, μ represents the effective carrying capacity of the system, the rate in which cancer cells destroy immune cells is represented by η, ϱ represents the killing impact on the infected cells.

In order to enrich the study of the system described in (9) and to contribute to the field of modeling using the techniques of fractional calculus, the fractional-order version of system (9) is given as [37]

$$\begin{cases} {}^{C}D^{\nu_1}C(t) = C\left[\alpha_1\left(1-\frac{C+S+R}{\mu}\right)-\delta_1 S\right], \\ {}^{C}D^{\nu_2}S(t) = S\left[\alpha_2\left(1-\frac{C+S+R}{\mu}\right)-\eta\delta_1 C-\delta_2 R\right], \\ {}^{C}D^{\nu_3}R(t) = \delta_2 SR-\varrho R, \end{cases} \tag{10}$$

where ν_1, ν_2, and ν_3 are the fractional-orders such that $\nu_i \in (0,1)$ for $i = 1,2,3$, and ${}^{C}D^{\nu}$ is the Caputo fractional derivative defined in [38].

Definition 3 *The Caputo fractional derivative of order $\nu \in \mathbb{R}^+$ of a continuous function $g(t) : [t_0, +\infty[\to \mathbb{R}$ is defined as*

$${}^{C}D^{\nu}_{t_0} g(t) = \frac{1}{\Gamma(m-\nu)} \int_{t_0}^{t} \frac{g^{(m)}(s)}{(t-s)^{\nu+1-m}} ds, \tag{11}$$

where $t > t_0$, $m-1 < \nu \leq m$, and $m = \lceil \nu \rceil$.

For $\nu_1 = \nu_2 = \nu_3 = \nu = 0.98$ and the parameter values listed in Table 1 under the initial conditions $(C(0), S(0), R(0)) = (678, 452, 0.25)$, the attractor of the commensurate fractional-order system (10) is shown in Figure 1(a). In addition, when $(\nu_1, \nu_2, \nu_3) = (0.96, 0.97, 0.98)$, the attractor of the non-commensurate fractional-order system (10) is shown in Figure 1(b).

Table 1. Parameter values of the continuous-time fractional-order system (10)

Parameter	Value
α_1	0.1785
α_2	0.03
δ_1	0.0001
δ_2	0.0005
η	0.01
μ	1500
ϱ	0.3

To simplify the study, we nondimensionalize the system (9) in order to obtain the scaled system. We set

$$u = \frac{C}{\mu}, \qquad v = \frac{S}{\mu}, \qquad w = \frac{R}{\mu}, \qquad \tau = \alpha_1 t, \tag{12}$$

where the new parameters are given by

$$b_{12} = \frac{\mu\delta_1}{\alpha_1}, \qquad b_{23} = \frac{\delta_2\mu}{\alpha_1}, \qquad b_{22} = \frac{\eta\delta_1\mu}{\alpha_1}, \qquad b_{31} = \frac{\delta_2\mu}{\alpha_1}, \qquad r = \frac{\alpha_2}{\alpha_1}, \qquad b_{32} = \frac{\varrho}{\alpha_1}. \tag{13}$$

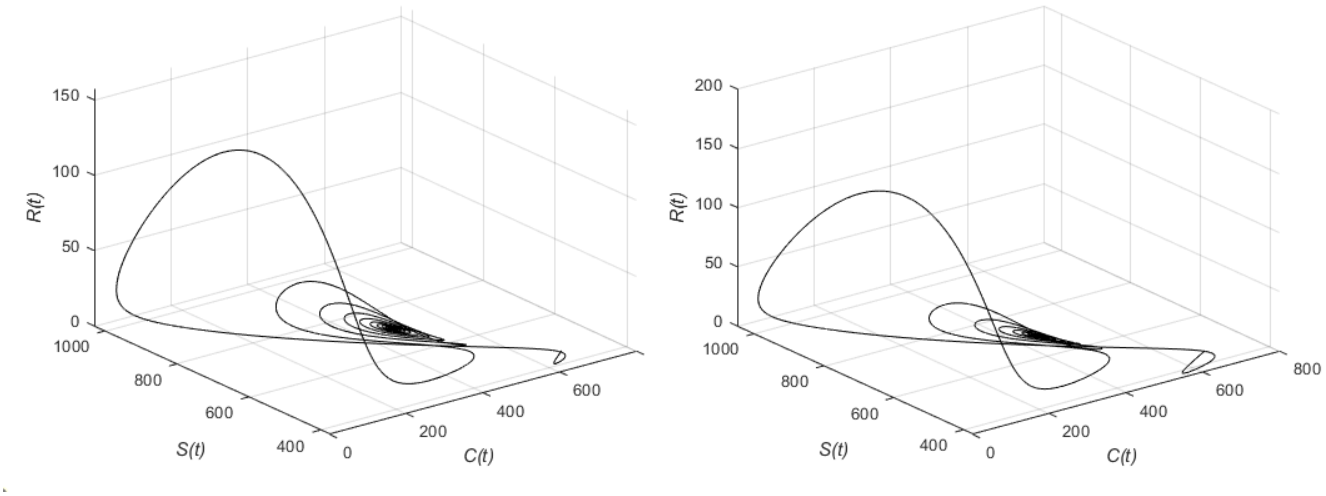

(a) commensurate fractional-order (b) non-commensurate fractional-order

Figure 1. Phase portrait of the fractional-order system (10)

Hence, the nondimensionalized system can be expressed as

$$\begin{cases} \frac{du}{d\tau} = u\left(1-(u+v+w)\right) - b_{12}uv, \\ \frac{dv}{d\tau} = rv\left(1-(u+v+w)\right) - b_{22}uv - b_{23}vw, \\ \frac{dw}{d\tau} = b_{31}vw - b_{32}w. \end{cases} \tag{14}$$

We can obtain the discrete fractional-order HIV-1 model with cancer cells related to AIDS by substituting the fractional derivatives ${}^{C}D^{\nu_i}$ with the Caputo-like discrete fractional difference operator ${}^{C}\Delta_{\alpha}^{\nu_i}$ as follows

$$\begin{cases} {}^{C}\Delta_{\alpha}^{\nu_1}u(\tau) = u(\tau+\nu_1-1)(1-(u(\tau+\nu_1-1)+v(\tau+\nu_1-1)+w(\tau+\nu_1-1)) \\ \qquad\qquad -b_{12}u(\tau+\nu_1-1)v(\tau+\nu_1-1), \\ {}^{C}\Delta_{\alpha}^{\nu_2}v(\tau) = rv(\tau+\nu_2-1)\left(1-(u(\tau+\nu_2-1)+v(\tau+\nu_2-1)+w(\tau+\nu_2-1))\right) \\ \qquad\qquad -b_{22}u(\tau+\nu_2-1)v(\tau+\nu_2-1)-b_{23}v(\tau+\nu_2-1)w(\tau+\nu_2-1), \\ {}^{C}\Delta_{\alpha}^{\nu_3}w(\tau) = b_{31}v(\tau+\nu_3-1)w(\tau+\nu_3-1)-b_{32}w(\tau+\nu_3-1). \end{cases} \tag{15}$$

For simplification, we will replace u, v, and w by x, y, and z, respectively. Using Theorem 1 with $\alpha = 0$, the numerical solution of the discrete fractional-order system (15) is given by

$$\begin{cases} x(n) = x(0) + \frac{1}{\Gamma(\nu_1)}\sum_{s=1}^{n}\frac{\Gamma(n-s+\nu_1)}{\Gamma(n-s+1)}(x(s-1)(1-(x(s-1)+y(s-1)+z(s-1))) \\ \qquad -b_{12}x(s-1)y(s-1)), \\ y(n) = y(0) + \frac{1}{\Gamma(\nu_2)}\sum_{s=1}^{n}\frac{\Gamma(n-s+\nu_2)}{\Gamma(n-s+1)}(ry(s-1)(1-(x(s-1)+y(s-1)+z(s-1))) \\ \qquad -b_{22}x(s-1)y(s-1)-b_{23}y(s-1)z(s-1)), \\ z(n) = z(0) + \frac{1}{\Gamma(\nu_3)}\sum_{s=1}^{n}\frac{\Gamma(n-s+\nu_3)}{\Gamma(n-s+1)}\left(b_{31}y(s-1)z(s-1)-b_{32}z(s-1)\right), \end{cases} \tag{16}$$

where $x(n)$, $y(n)$, and $z(n)$ represent the number of cancer cells, healthy cells, and HIV-infected cells respectively.b_{12}, b_{22}, b_{23}, b_{31}, b_{32}, and r are constant positive parameters.

4 Dynamics of the fractional-order discrete system

This section focuses on the analysis of the dynamics of the discrete fractional-order HIV-1 model with cancer cells related to AIDS (15) in both commensurate and non-commensurate fractional orders.

Case 1. Commensurate fractional-order

Existence and stability of equilibria

In this part, we study the existence and stability of equilibria in the fractional-order system (15). The equilibrium points of the fractional-order system (15) are the solutions of the following system of equations:

$$\begin{cases} x\left(1-(x+y+z)\right)-b_{12}xy=0, \\ ry\left(1-(x+y+z)\right)-b_{22}xy-b_{23}yz=0, \\ b_{31}yz-b_{32}z=0. \end{cases} \tag{17}$$

If we assume that $b_{22} \neq b_{23}$, the equilibrium points of (15) are:

$$\begin{aligned} F_0 &= (0,0,0), \quad F_1=(1,0,0), \quad F_2=(0,1,0), \quad F_3=\left(0,\frac{b_{32}}{b_{31}},\frac{-3r}{r+b_{23}}\right), \\ F_4 &= \left(\frac{rb_{12}}{rb_{12}+b_{22}b_{12}+b_{22}},\frac{b_{22}}{rb_{12}+b_{22}b_{12}+b_{22}},0\right), \\ F_5 &= \left(\frac{b_{31}b_{23}-(b_{23}b_{12}+rb_{12}+b_{23})b_{32}}{b_{31}(b_{23}-b_{22})},\frac{b_{32}}{b_{31}},\frac{(rb_{12}+b_{22}b_{12}+b_{22})b_{32}-b_{31}b_{22}}{b_{31}(b_{23}-b_{22})}\right). \end{aligned}$$

Fix $b_{31}=0.01$, $b_{22}=0.08$, $b_{23}=0.01$, $b_{12}=0.08$, $b_{32}=0.04$, $r=3.4$, the fixed points and the corresponding eigenvalues are shown in Table 2.

Table 2. Equilibria of the fractional-order discrete system (15)

Fixed points	Eigenvalues
F_0	$\lambda_1=1,\ \lambda_2=3.4,\ \lambda_3=-0.04$
F_1	$\lambda_1=-1,\ \lambda_2=-0.08,\ \lambda_3=-0.04$
F_2	$\lambda_1=-3.4,\ \lambda_2=-1.08,\ \lambda_3=-0.03$
F_3	$\lambda_1=0.0299,\ \lambda_2=-13.6299,\ \lambda_3=-0.3288$
F_4	$\lambda_1=-1.5569,\ \lambda_2=0.039,\ \lambda_3=-0.0378$
F_5	$\lambda_1=-30.4586,\ \lambda_2=0.8061,\ \lambda_3=0.0353$

The equilibrium points F_0, F_3, F_4, F_5 have real positive eigenvalue, then the condition $\arg(\lambda_j) > \nu\frac{\pi}{2}$ is not achieved. Based on Theorem 2, the equilibrium points F_0, F_3, F_4, and F_5 are unstable. Also, the equilibrium point F_2 is unstable. We found that the corresponding eigenvalues are $\lambda_1=-3.4$, $\lambda_2=-1.08$, $\lambda_3=-0.03$. Then we have $\arg(\lambda_1)=\pi > \nu\frac{\pi}{2}$, but any value of ν can verify $|\lambda_1| < \left(2\cos\frac{|\arg(\lambda_1)|-\pi}{2-\nu}\right)^{\nu}$.

Theorem 3 *The equilibrium point F_1 of the fractional-order discrete system (15) is locally asymptotically stable.*

Proof The Jacobian matrix of the system (15) evaluated at the equilibrium point (x, y, z) is given by

$$J = \begin{pmatrix} 1-2x-(y+z)-b_{12}y & -(1+b_{12})x & -x \\ -(r+b_{22})y & r(1-(x+y+z))-ry-b_{22}x-b_{23}z & -(r+b_{23})y \\ 0 & b_{31}z & b_{31}y-b_{32} \end{pmatrix}. \tag{18}$$

The eigenvalues of the matrix J at F_1 are $\lambda_1 = -1$, $\lambda_2 = -0.08$, $\lambda_3 = -0.04$. Using Theorem 2, the equilibrium point F_1 is asymptotically stable.

Bifurcation diagrams and maximum Lyapunov exponent

This part focuses on the investigation of the dynamics properties of the commensurate fractional-order discrete HIV-1 model (15) and the influence of the parameters on the dynamic behavior of system (15). Fix $b_{31} = 0.01$, $b_{22} = 0.08$, $b_{23} = 0.01$, $b_{12} = 0.08$, $b_{32} = 0.04$ and vary r in the interval $[2, 3.8]$ when $\nu = 0.4$, then when $\nu = 0.92$ under the initial conditions $(x(0), y(0), z(0)) = (0.1, 0.2, 0.25)$. The bifurcation diagrams of the discrete system (15) are shown in Figure 2. We see that when $\nu = 0.4$, the system is stable for $r \in [2, 3.23]$, but when r increases, the system (15) exhibits chaotic dynamics in the range $r \in [3.23, 3.8]$. For $\nu = 0.92$, the dynamics of the system are complex, and the chaotic behavior is dominated. Clearly, when $r \in [2, 2.6]$, the system (15) is periodic, but when $r \in [2.6, 3.6]$, the system (15) exhibits chaotic behavior, but when r increases, the chaotic behavior gradually disappears.

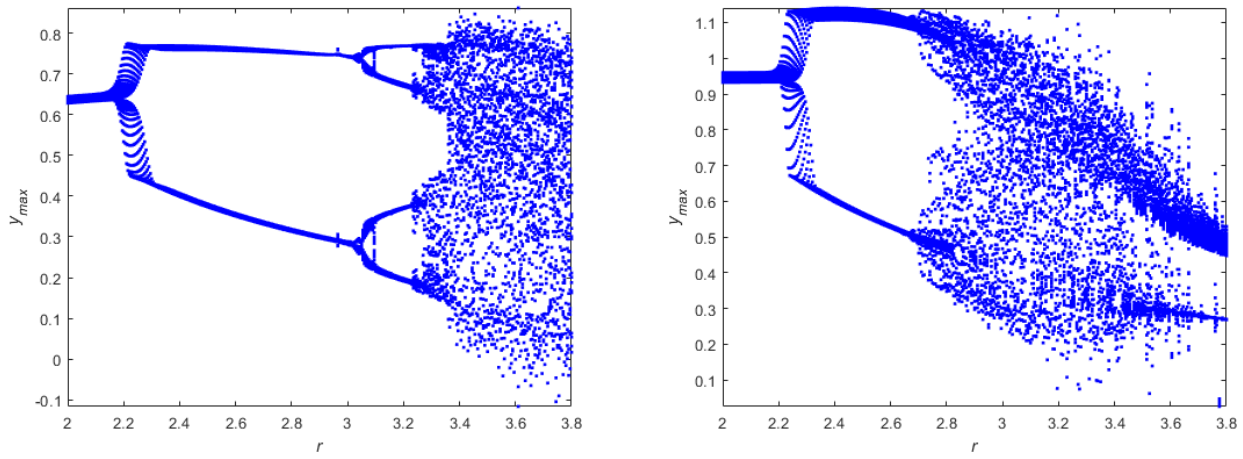

(a) for $\nu = 0.4$ (b) for $\nu = 0.92$

Figure 2. Bifurcation diagrams of the fractional-order system (15) as r varies

Now, we investigate the influence of the fractional order on the dynamics of the fractional-order system (15). Figure 3 represents the bifurcation diagram of the commensurate fractional-order discrete system (15) for the parameter values $b_{31} = 0.01$, $b_{22} = 0.08$, $b_{23} = 0.01$, $b_{12} = 0.08$, $b_{32} = 0.04$, and $r = 3.4$. As can be observed, the system (15) is periodic at first, but if ν increases, the dynamics of the system become unstable with the appearance of a chaotic state in the range $\nu \in [0.14, 1]$.

We can also investigate the chaotic behavior in the system (15) by exploiting the maximum Lyapunov exponent. It should be noted that the maximum Lyapunov exponent can be approximated using the Jacobian matrix algorithm [39]. We set $r_0 = (x(0), y(0), z(0))^T$, the Lyapunov exponent

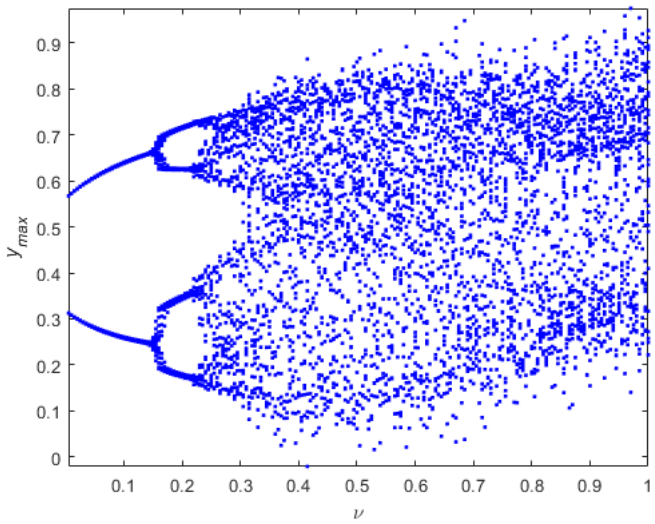

Figure 3. Bifurcation diagram of the fractional-order system (15) as ν varies

is defined as

$$\lambda_i(r_0) = \lim_{n\to\infty} \frac{1}{n} \ln|\lambda_i^{(n)}|, \quad i = 1, 2, 3, \tag{19}$$

where λ_i $(i = 1, 2, 3)$ are the eigenvalues of the tangent map J_n given by

$$J_n = \begin{pmatrix} \theta_1(n) & \theta_2(n) & \theta_3(n) \\ \theta_4(n) & \theta_5(n) & \theta_6(n) \\ \theta_7(n) & \theta_8(n) & \theta_9(n) \end{pmatrix}, \tag{20}$$

where

$$\begin{aligned}
\theta_1(n) &= \theta_1(0) + \frac{1}{\Gamma(\nu)} \sum_{s=1}^{n} \frac{\Gamma(n-s+\nu)}{\Gamma(n-s+1)} (\theta_1(s-1)(1-2x(s-1)-y(s-1)-z(s-1)-b_{12}y(s-1)) \\
&\quad +\theta_4(s-1)(-x(s-1)-b_{12}x(s-1))-\theta_7(s-1)x(s-1)), \\
\theta_2(n) &= \theta_2(0) + \frac{1}{\Gamma(\nu)} \sum_{s=1}^{n} \frac{\Gamma(n-s+\nu)}{\Gamma(n-s+1)} (\theta_2(s-1)(1-2x(s-1)-y(s-1)-z(s-1)-b_{12}y(s-1)) \\
&\quad +\theta_5(s-1)(-x(s-1)-b_{12}x(s-1))-\theta_8(s-1)x(s-1)), \\
\theta_3(n) &= \theta_3(0) + \frac{1}{\Gamma(\nu)} \sum_{s=1}^{n} \frac{\Gamma(n-s+\nu)}{\Gamma(n-s+1)} (\theta_3(s-1)(1-2x(s-1)-y(s-1)-z(s-1)-b_{12}y(s-1)) \\
&\quad +\theta_6(s-1)(-x(s-1)-b_{12}x(s-1))-\theta_9(s-1)x(s-1)), \\
\theta_4(n) &= \theta_4(0) + \frac{1}{\Gamma(\nu)} \sum_{s=1}^{n} \frac{\Gamma(n-s+\nu)}{\Gamma(n-s+1)} (\theta_1(s-1)(-ry(s-1)-b_{22}y(s-1)) + \theta_4(s-1)(r-rx(s-1) \\
&\quad -2ry(s-1)-rz(s-1)-b_{22}x(s-1)-b_{23}z(s-1)) + \theta_7(s-1)(-ry(s-1)-b_{23}y(s-1)), \\
\theta_5(n) &= \theta_5(0) + \frac{1}{\Gamma(\nu)} \sum_{s=1}^{n} \frac{\Gamma(n-s+\nu)}{\Gamma(n-s+1)} (\theta_2(s-1)(-ry(s-1)-b_{22}y(s-1)) + \theta_5(s-1)(r-rx(s-1) \\
&\quad -2ry(s-1)-rz(s-1)-b_{22}x(s-1)-b_{23}z(s-1)) + \theta_8(s-1)(-ry(s-1)-b_{23}y(s-1)),
\end{aligned}$$

$$
\begin{aligned}
\theta_6(n) &= \theta_6(0) + \frac{1}{\Gamma(\nu)} \sum_{s=1}^{n} \frac{\Gamma(n-s+\nu)}{\Gamma(n-s+1)} (\theta_3(s-1)(-ry(s-1) - b_{22}y(s-1)) \\
&\quad + \theta_6(s-1)(r - rx(s-1) - 2ry(s-1) - rz(s-1) - b_{22}x(s-1) - b_{23}z(s-1)) \\
&\quad + \theta_9(s-1)(-ry(s-1) - b_{23}y(s-1)), \\
\theta_7(n) &= \theta_7(0) + \frac{1}{\Gamma(\nu)} \sum_{s=1}^{n} \frac{\Gamma(n-s+\nu)}{\Gamma(n-s+1)} (b_{31}\theta_4(s-1)z(s-1) + \theta_7(s-1)(b_{31}y(s-1) - b_{32}), \\
\theta_8(n) &= \theta_8(0) + \frac{1}{\Gamma(\nu)} \sum_{s=1}^{n} \frac{\Gamma(n-s+\nu)}{\Gamma(n-s+1)} (b_{31}\theta_5(s-1)z(s-1) + \theta_8(s-1)(b_{31}y(s-1) - b_{32}), \\
\theta_9(n) &= \theta_9(0) + \frac{1}{\Gamma(\nu)} \sum_{s=1}^{n} \frac{\Gamma(n-s+\nu)}{\Gamma(n-s+1)} (b_{31}\theta_6(s-1)z(s-1) + \theta_9(s-1)(b_{31}y(s-1) - b_{32}),
\end{aligned}
$$

with $\theta_1(0) = \theta_5(0) = \theta_9(0) = 1$, $\theta_i(0) = 0$ $(i = 2, 3, 4, 6, 7, 8)$. Figure 4(a) and Figure 4(b) show the maximum Lyapunov exponent of the fractional-order system (15) with respect to parameter r under the parameter values $b_{31} = 0.01$, $b_{22} = 0.08$, $b_{23} = 0.01$, $b_{12} = 0.08$, $b_{32} = 0.04$, and the fractional-orders $\nu = 0.4$ and $\nu = 0.92$ respectively. In Figure 4(a), when $r \in [2, 3.8]$, we see that the MLE is equal to zero when $r \in [2, 3.22]$ and the system (15) is periodic, but when r increases, the MLE has positive values, meaning that the discrete fractional-order system (15) transitions from a periodic state to a chaotic state. In Figure 4(b), the MLE of the system (15) is negative at the minimum values of r, then the system (15) is periodic. In addition, when $r \in [2.6, 3.4]$, the MLE is positive, then the system (15) is chaotic. As can be observed, when r increases, the MLE takes positive and negative values, and then the appearance of periodic orbits in the chaotic regions is confirmed. Now, we analyze the MLE of the discrete fractional-order system (15) when the

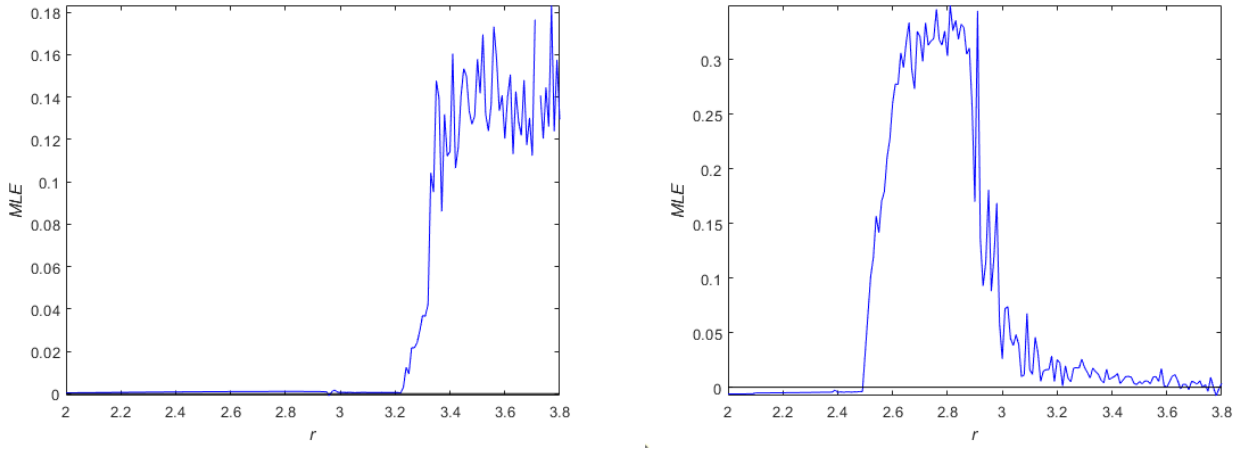

(a) for $\nu = 0.4$ (b) for $\nu = 0.92$

Figure 4. MLE spectrum of the fractional-order system (15) as r varies

fractional-order varies. Figure 5 represents the maximum Lyapunov exponent when ν ranges from 0 to 1. As can be observed, the MLE of system (15) is equal to zero when $\nu \in (0, 0.15]$, and then the system (15) remains in periodic state, but when $\nu \geq 0.15$, the MLE is positive, and then the system (15) exhibits chaotic behavior. The attractor of the fractional-order discrete system (15) for various ν-values is depicted in Figure 6.

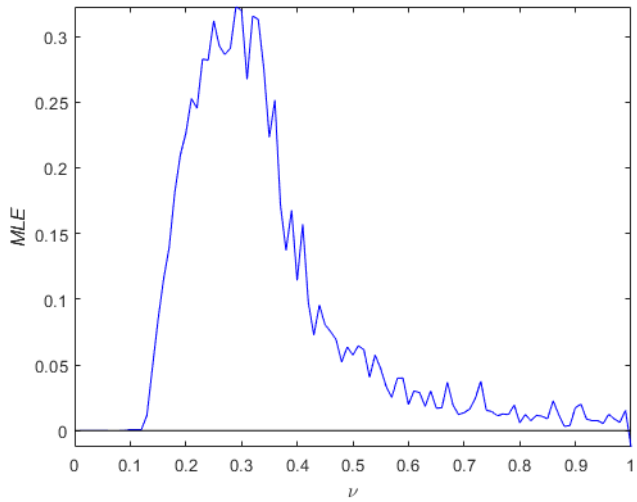

Figure 5. MLE spectrum of the fractional-order system (15) as ν varies

Case2. Non-commensurate fractional-order

Now, we study the dynamic behavior of the system (15) in the non-commensurate fractional-order case. Fix $b_{31} = 0.01$, $b_{22} = 0.08$, $b_{23} = 0.01$, $b_{12} = 0.08$, $b_{32} = 0.04$, $r = 3.4$, $\nu_1 = 0.21$, $\nu_3 = 0.34$, and vary ν_2 from 0 to 1. Figure 7 shows the bifurcation diagram and its corresponding MLE spectrum. By examining the MLE and the bifurcation diagram displayed in Figure 7, we find that the fractional-order discrete system (15) may experience two scenarios according to the values of ν_2. When $\nu_2 \in [0, 0.18]$, the MLE is negative or equal to zero, then the state of system (15) is periodic, but when $\nu_2 \in [0.18, 0.91]$, the MLE is positive, then the system (15) exhibits robust chaos across this parameter ν_2 range. Finally, when $\nu_2 > 0.91$, the MLE is equal to zero once again, meaning that the system (15) is periodic.

Now, we study the dynamics of the discrete incommensurate fractional-order system (15) when ν_1 varies. Figure 8 represents the bifurcation diagram and its corresponding MLE spectrum for $\nu_2 = 0.3$, and $\nu_3 = 0.4$. We see that the MLE is positive when $\nu_1 \in [0, 0.4]$, and then the system (15) exhibits robust chaos, but when $\nu_1 > 0.4$, the chaotic state arises with the appearance of the periodic state, as shown by the MLE's oscillation between positive and negative values.

Moreover, to show the dynamic behavior of the non-commensurate fractional-order system (15), we vary ν_3 when $\nu_1 = 0.5$, and $\nu_2 = 0.6$. Figure 9 shows the bifurcation diagram and the MLE spectrum of the fractional-order system (15). As we can see, at the minimum values of ν_3, the discrete non-commensurate fractional-order system (15) has a negative or zero MLE, but when ν_3 increases, the MLE has strictly positive values, meaning that the system transitions from a periodic state to a chaotic state.

To provide further clarification, the phase portrait of the non-commensurate fractional-order system (15) is shown in Figure 10 for different values of (ν_1, ν_2, ν_3).

5 0-1 test and complexity of the fractional-order system

Test 0-1 for Chaos

The 0-1 test is an efficient technique to detect chaos in discrete fractional-order systems. We review the steps of this algorithm [40]. Based on the state $x(n)$ in Eq. (16), we construct the translation

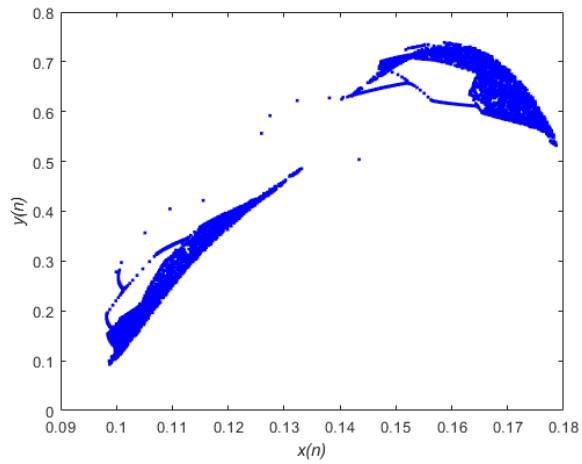

(a) for $\nu = 0.12$

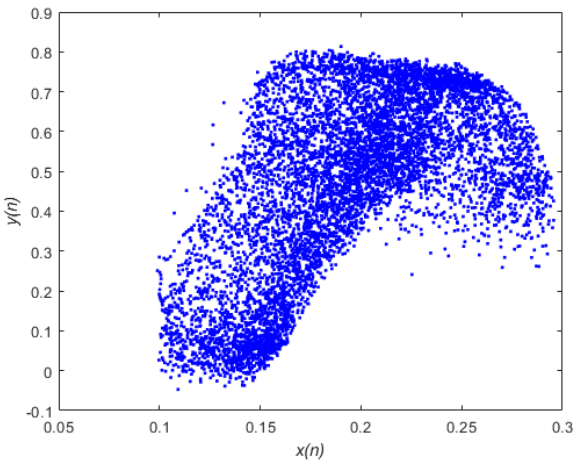

(b) for $\nu = 0.24$

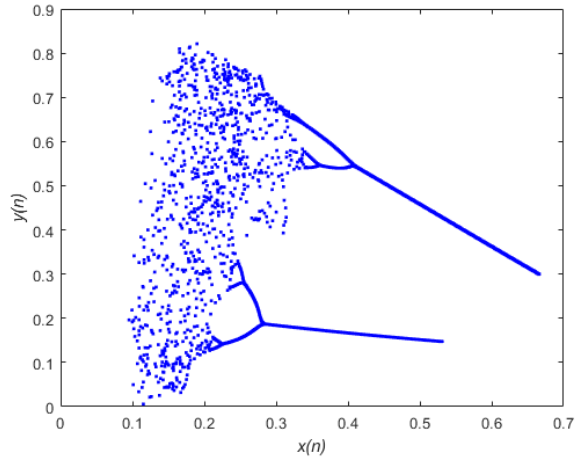

(c) for $\nu = 0.36$

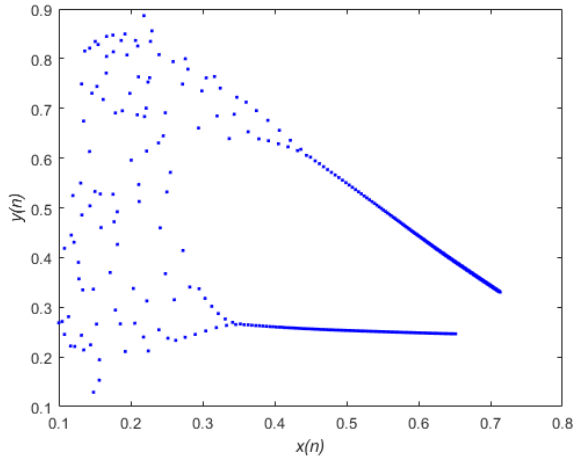

(d) for $\nu = 0.75$

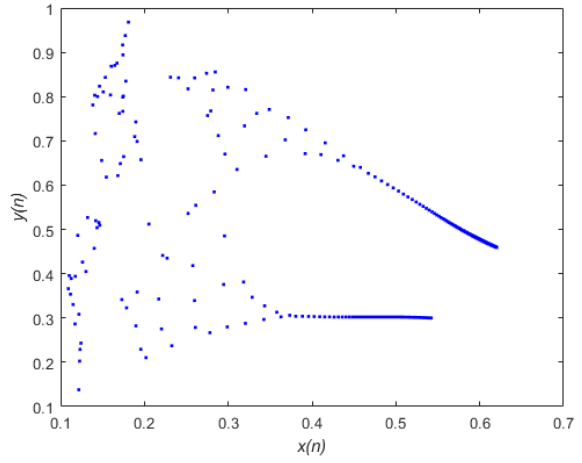

(e) for $\nu = 0.89$

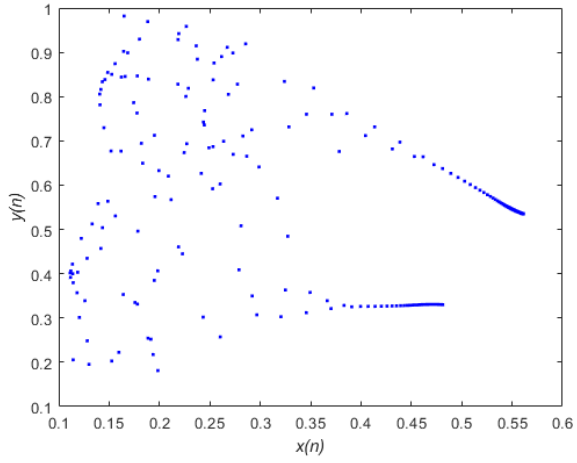

(f) for $\nu = 0.96$

Figure 6. Attractor of the fractional-order discrete system (15) for different values of ν

components p_c and q_c as follows

$$p_c(n) = \sum_{k=1}^{n} x(k)\cos(kc), \qquad q_c(n) = \sum_{k=1}^{n} x(k)\sin(kc), \tag{21}$$

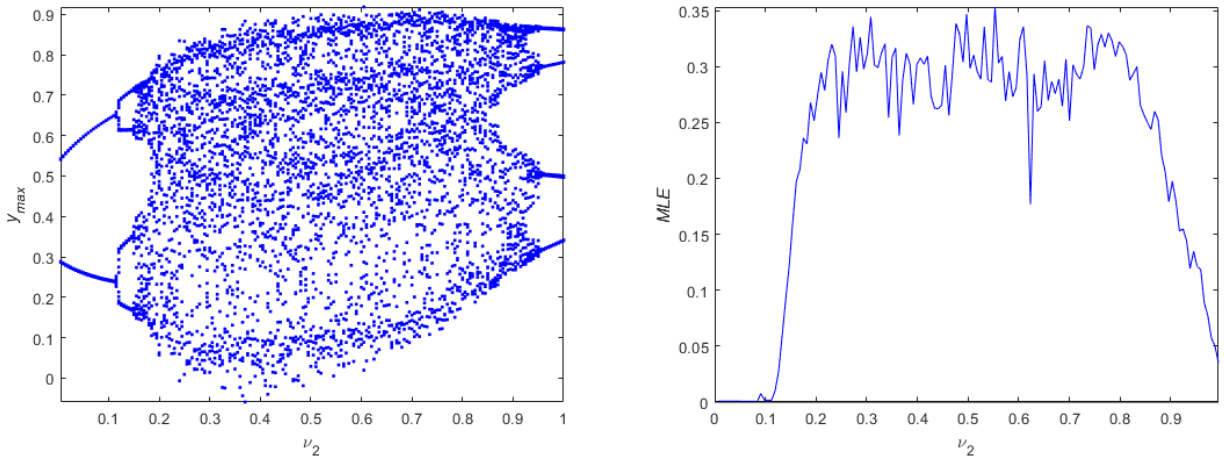

(a) Bifurcation diagram as ν_2 varies (b) The MLE spectrum as ν_2 varies

Figure 7. Bifurcation and MLE spectrum diagrams for ν_2

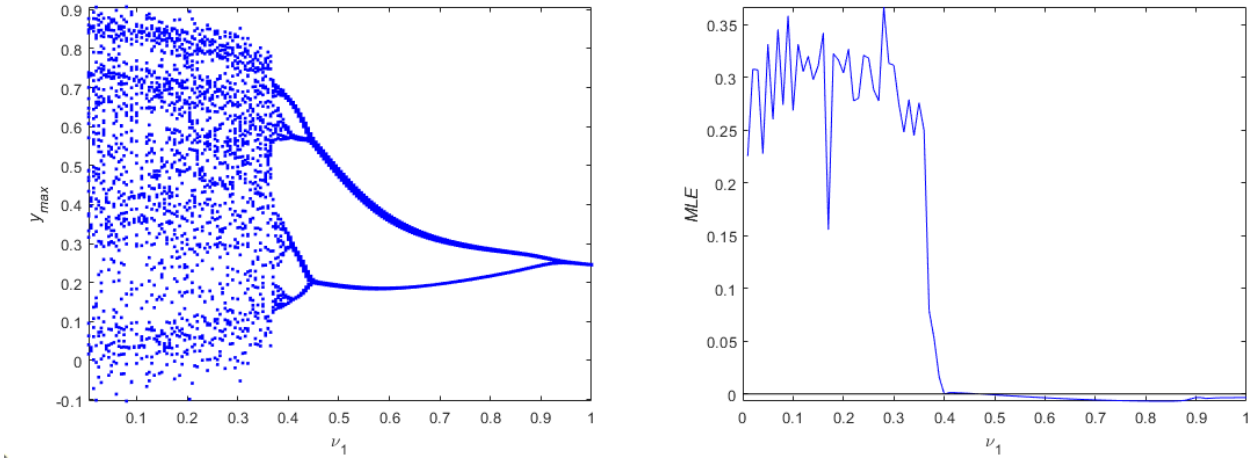

(a) Bifurcation diagram as ν_1 varies (b) The MLE spectrum as ν_1 varies

Figure 8. Bifurcation and MLE spectrum diagrams for ν_1

where c is a random constant selected from $(0, \pi)$. We can plot p_c and q_c to verify if the chaotic behavior appears when the bounded motions of p_c and q_c imply regular dynamics, whereas the asymptotic Brownian movement implies chaotic dynamics. Figure 11 shows the results.

C_0 complexity

We can evaluate the complexity of a discrete chaotic system via the C_0 algorithm. Assume that $x(j)$ $(j = 0, 1, \ldots, L-1$, where $L \geq 1$ is a sequence of data selected from the discrete system (15). The corresponding discrete Fourier transformation for this data set is given by

$$X_L(k) = \sum_{j=0}^{L-1} x(j) \exp\left[\frac{-2\pi ijk}{L}\right], \tag{22}$$

where $k = 0, 1, \ldots, L-1$, and i is the imaginary unit. Next, the mean of X_L is obtained as

$$M_L = \frac{1}{L} \sum_{k=0}^{L-1} |X_L(k)|^2. \tag{23}$$

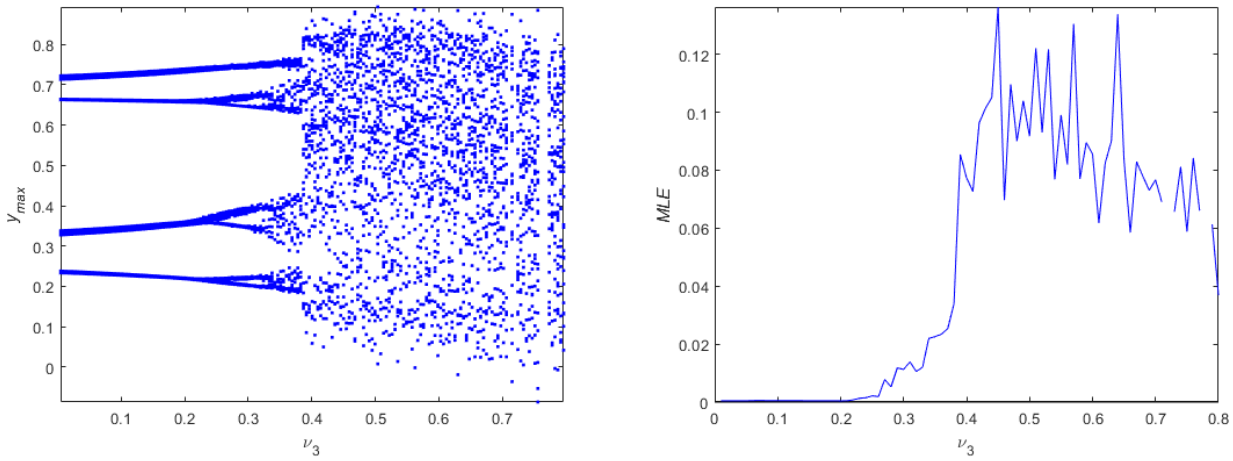

(a) Bifurcation diagram as ν_3 varies

(b) The MLE spectrum as ν_3 varies

Figure 9. Bifurcation and MLE spectrum diagrams for ν_3

A control parameter υ is introduced as

$$\tilde{X}_L(k) = \begin{cases} X(k) & \text{if} \quad |X_L(k)|^2 > \upsilon M_L, \\ 0 & \text{if} \quad |X_L(k)|^2 \leq \upsilon M_L. \end{cases} \tag{24}$$

The inverse discrete Fourier transformation of $\tilde{X}_L$ is given by

$$\tilde{x}(j) = \frac{1}{L} \sum_{k=0}^{L-1} \tilde{X}_L(k) \exp[\frac{2\pi i j k}{L}], \tag{25}$$

where $j = 0, 1, \ldots, L-1$. Finally, the C_0 complexity is defined as [41]

$$C_0(x, \upsilon, L) = \frac{\sum_{j=0}^{L-1} |x(j) - \tilde{x}(j)|^2}{\sum_{j=0}^{L-1} |x(j)|^2}. \tag{26}$$

Fix $b_{31} = 0.01$, $b_{22} = 0.08$, $b_{23} = 0.01$, $b_{12} = 0.08$, $b_{32} = 0.04$, $r = 3.4$, $\nu_1 = 0.21$, $\nu_3 = 0.34$, the C_0 complexity with respect to fractional-order ν_2 is shown in Figure 12. As can be observed, the complexity of the fractional-order system (15) changes as we vary ν_2, which agrees well with the findings of the bifurcation diagram and maximum Lyapunov exponent.

Approximate entropy

In the dynamical analysis of nonlinear chaotic systems, approximate entropy (ApEn) is an efficient technique that allows us to measure the level of complexity in chaotic systems. In brief, we review the steps to evaluate the approximate entropy for the fractional-order system (15). We select a sequence of data $x(j)$ $(j = 1, 2, \ldots, N)$ from the system (15), then we construct a sequence of vectors $\mu(1), \mu(2), \ldots, \mu(N - m + 1)$ as: $\mu(j) = [x(j), x(j+1), x(j+2), \ldots, x(j+m-1)]$, and $\mu(i) = [x(i), x(i+1), x(i+2), \ldots, x(i+m-1)]$, where m is a positive integer representing the embedding dimension. The distance between two vectors is given by

$$d\left(\mu(j), \mu(i)\right) = \max\{|x(j+s-1) - x(i+s-1)|\}, \quad s = 1, 2, \ldots, m. \tag{27}$$

We take a non-negative number r and we denote by L the number of j where $d\left(\mu(j), \mu(i)\right) \leq r$, the approximate entropy is defined as [42]

$$\text{ApEn} = \Lambda^m(r) - \Lambda^{m+1}(r), \tag{28}$$

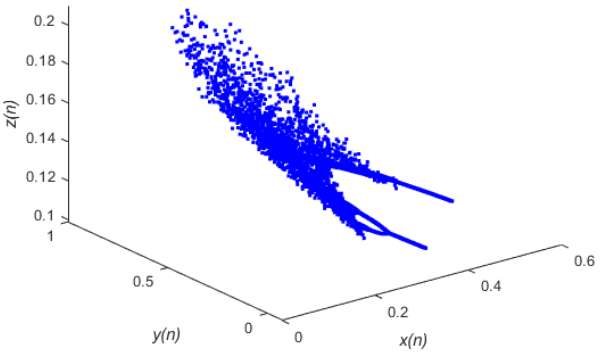

(a) for $(\nu_1, \nu_2, \nu_3) = (0.3, 0.3, 0.4)$

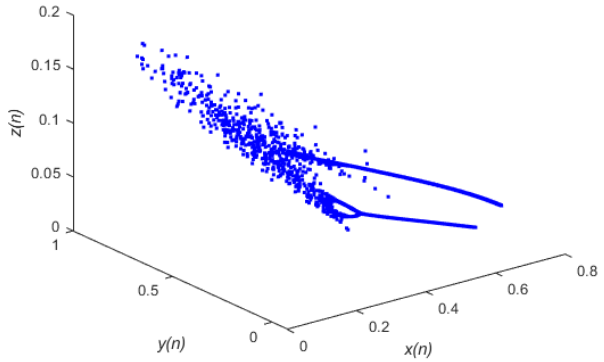

(b) for $(\nu_1, \nu_2, \nu_3) = (0.4, 0.55, 0.6)$

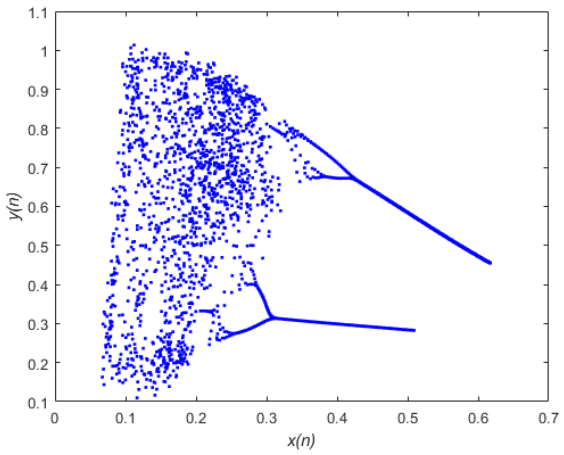

(c) for $(\nu_1, \nu_2, \nu_3) = (0.6, 0.96, 0.58)$

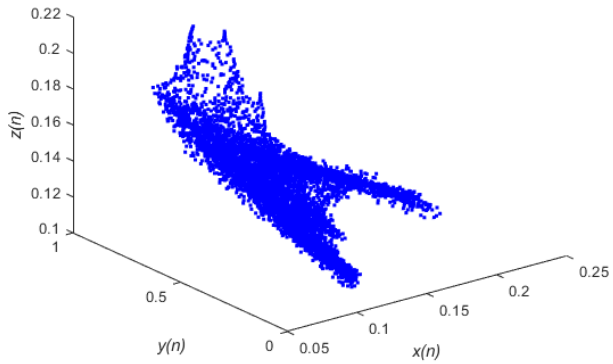

(d) for $(\nu_1, \nu_2, \nu_3) = (0.4, 0.9, 0.4)$

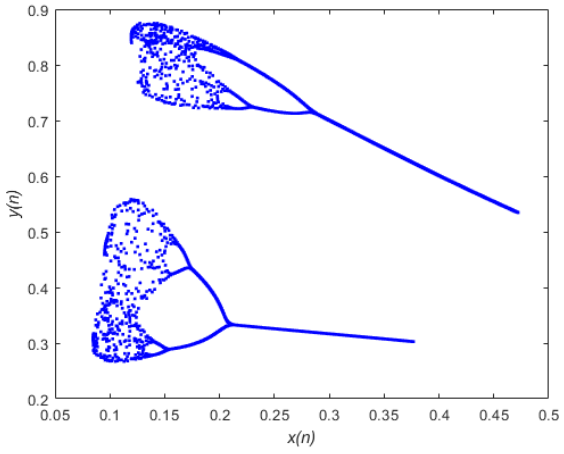

(e) for $(\nu_1, \nu_2, \nu_3) = (0.6, 0.9, 0.4)$

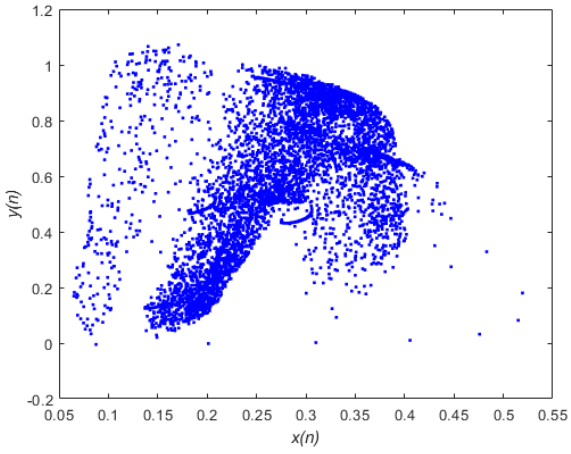

(f) for $(\nu_1, \nu_2, \nu_3) = (0.36, 0.98, 0.7)$

Figure 10. Attractor of the non-commensurate fractional-order system (15)

where $\Lambda^m(r)$ is determined as

$$\Lambda^m(r) = \frac{1}{N-m+1} \sum_{j=1}^{N-m+1} \log Q_j^m(r), \tag{29}$$

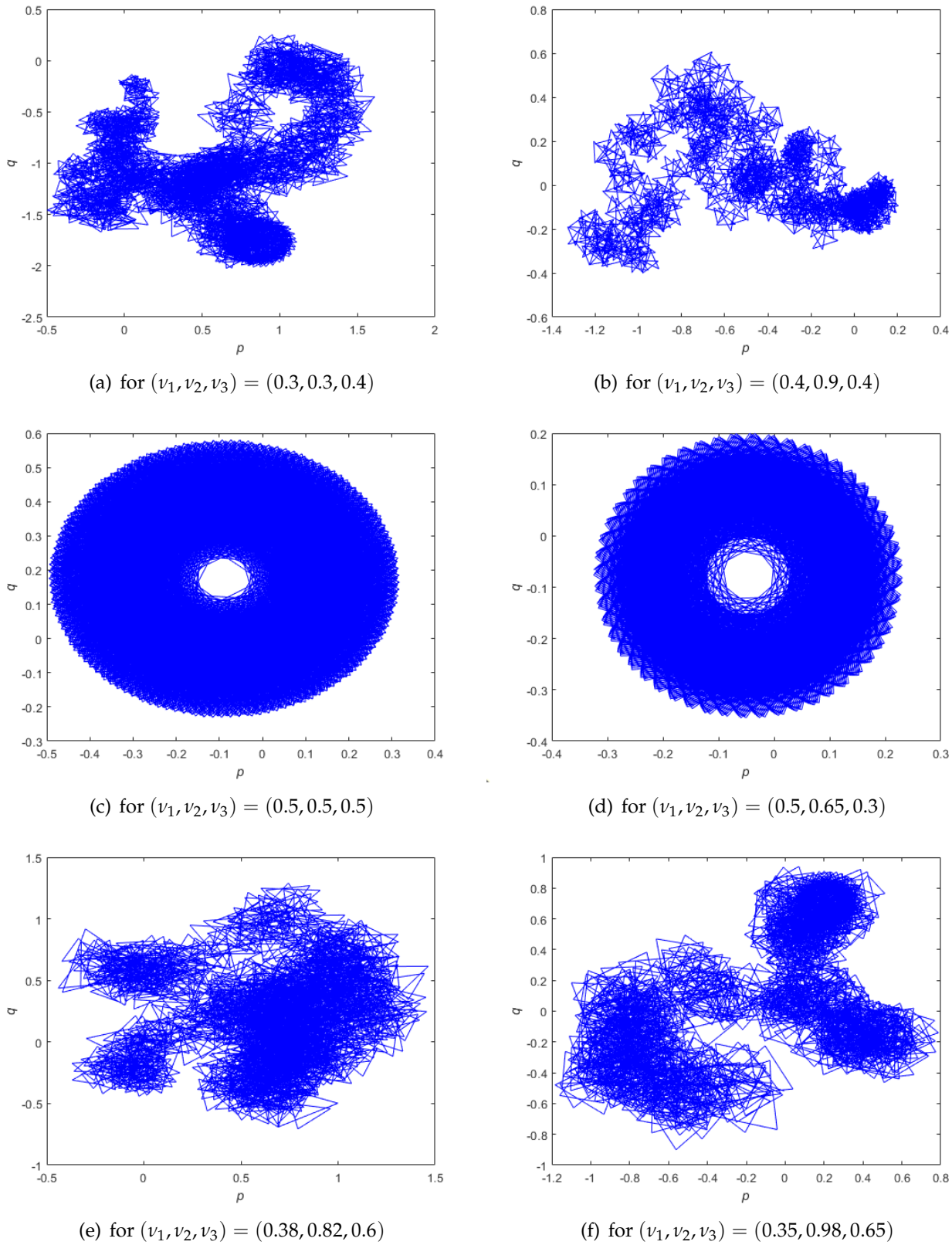

(a) for $(\nu_1, \nu_2, \nu_3) = (0.3, 0.3, 0.4)$

(b) for $(\nu_1, \nu_2, \nu_3) = (0.4, 0.9, 0.4)$

(c) for $(\nu_1, \nu_2, \nu_3) = (0.5, 0.5, 0.5)$

(d) for $(\nu_1, \nu_2, \nu_3) = (0.5, 0.65, 0.3)$

(e) for $(\nu_1, \nu_2, \nu_3) = (0.38, 0.82, 0.6)$

(f) for $(\nu_1, \nu_2, \nu_3) = (0.35, 0.98, 0.65)$

Figure 11. Dynamics of the translation components p_c and q_c

and $Q_j^m(r)$ is given by

$$Q_j^m(r) = \frac{L}{N - m + 1}. \tag{30}$$

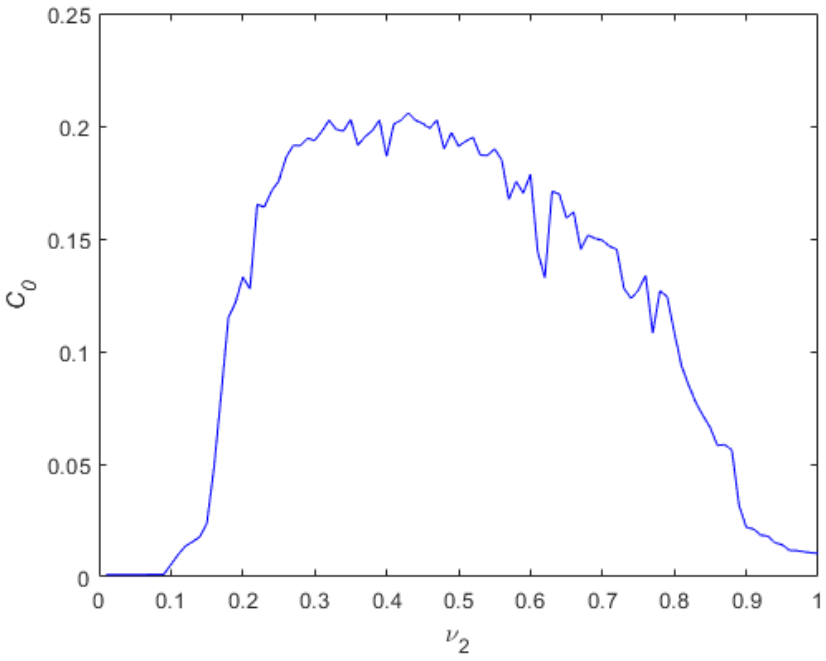

Figure 12. C_0 complexity of the fractional-order system (15) as ν_2 varies

Fix $b_{31} = 0.01$, $b_{22} = 0.08$, $b_{23} = 0.01$, $b_{12} = 0.08$, $b_{32} = 0.04$, $r = 3.4$, $\nu_1 = 0.21$, and $\nu_3 = 0.34$, the approximate entropy of the fractional-order system (15) with respect to ν_2 is shown in Figure 13. As can be observed, the approximate entropy of the system (15) changes when we vary ν_2, which agrees well with the findings derived in Section 4.

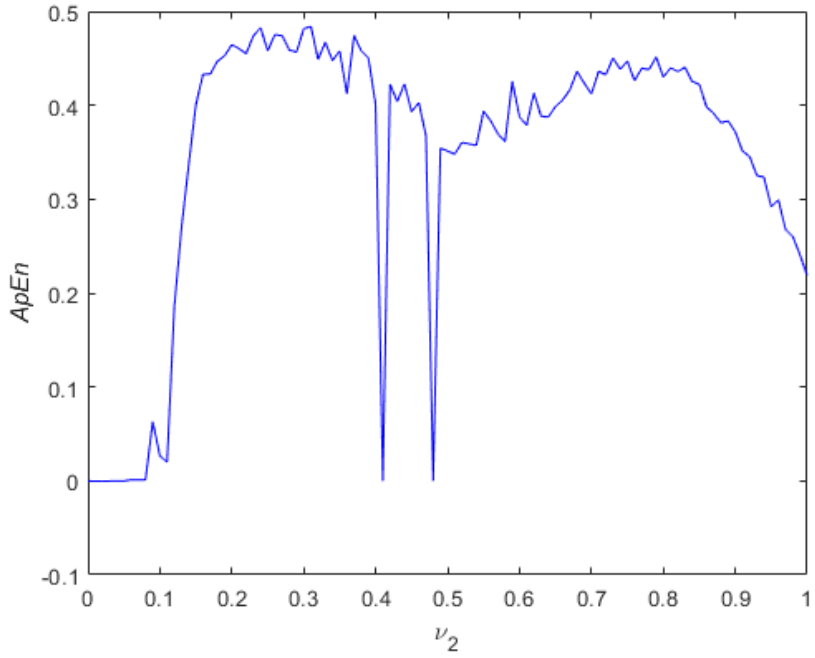

Figure 13. Approximate entropy of the fractional-order system (15) as ν_2 varies

6 Control scheme for the discrete fractional-order chaotic system

This section is devoted to the chaos control in the discrete commensurate fractional-order system (15) where an active fractional-order controller is designed.
The fractional-order system (15) with the controller $(u_1, u_2, u_3)^T$ is described as

$$\begin{cases} {}^{C}\Delta_{\theta}^{\nu} x(\tau) = x(\tau+\nu-1)\left(1-(x(\tau+\nu-1)+y(\tau+\nu-1)+z(\tau+\nu-1))\right) \\ \qquad\qquad -b_{12}x(\tau+\nu-1)y(\tau+\nu-1)+u_1(\tau+\nu-1), \\ {}^{C}\Delta_{\theta}^{\nu} y(\tau) = ry(\tau+\nu-1)\left(1-(x(\tau+\nu-1)+y(\tau+\nu-1)+z(\tau+\nu-1))\right) \\ \qquad\qquad -b_{22}x(\tau+\nu-1)y(\tau+\nu-1)-b_{23}y(\tau+\nu-1)z(\tau+\nu-1)+u_2(\tau+\nu-1), \\ {}^{C}\Delta_{\theta}^{\nu} z(\tau) = b_{31}y(\tau+\nu-1)z(\tau+\nu-1)-b_{32}z(\tau+\nu-1)+u_3(\tau+\nu-1), \end{cases} \tag{31}$$

where $\tau \in \mathbb{N}(\alpha-\nu)+1$. Our goal is to design a suitable control law that guarantees that all states of the fractional-order system (15) converge towards zero asymptotically.

Theorem 4 *The discrete fractional-order chaotic system* (15) *is stabilized under the following* 3*-D control law*

$$\begin{cases} u_1(\tau) = x(\tau)\left(x(\tau)+y(\tau)+z(\tau)-2\right)+b_{12}x(\tau)y(\tau), \\ u_2(\tau) = ry(\tau)\left(x(\tau)+y(\tau)+z(\tau)\right)-4y(\tau)+b_{22}x(\tau)y(\tau)+b_{23}y(\tau)z(\tau), \\ u_3(\tau) = -0.96z(\tau)-b_{31}y(\tau)z(\tau). \end{cases} \tag{32}$$

Proof Substituting (32) into (31), we obtain

$$\begin{cases} {}^{C}\Delta_{\theta}^{\gamma} x(\tau) = -x(\tau+\nu-1), \\ {}^{C}\Delta_{\theta}^{\gamma} y(\tau) = (r-4)y(\tau+\nu-1), \\ {}^{C}\Delta_{\theta}^{\gamma} z(\tau) = -(b_{32}+0.96)z(\tau+\nu-1), \end{cases} \tag{33}$$

which can be expressed as

$${}^{C}\Delta_{\theta}^{\nu}\left(x(\tau),y(\tau),z(\tau)\right)^T = N\left(x(\tau),y(\tau),z(\tau)\right)^T, \tag{34}$$

where

$$N = \begin{pmatrix} -1 & 0 & 0 \\ 0 & r-4 & 0 \\ 0 & 0 & -(b_{32}+0.96) \end{pmatrix}. \tag{35}$$

Then, the eigenvalues of the matrix N are $\lambda_1 = -1$, $\lambda_2 = r-4$, $\lambda_3 = -(b_{32}+0.96)$. It is easy to verify that λ_j $(j = 1,2,3)$ satisfy

$$|\arg\lambda_j| = \pi > \nu\frac{\pi}{2}, \quad \text{and} \quad |\lambda_j| < \left(2\cos\frac{|\arg\lambda_j|-\pi}{2-\nu}\right)^{\nu}, \quad \nu \in (0,1). \tag{36}$$

Therefore, using Theorem 2, we can conclude that the zero equilibrium of (34) is asymptotically stable. Thus, the stabilization of the fractional-order discrete system (31) is achieved.

For numerical simulations, the parameter values are selected as $b_{31} = 0.01$, $b_{22} = 0.08$, $b_{23} = 0.01$, $b_{12} = 0.08$, $b_{32} = 0.04$, $r = 3.4$, and the fractional-order as $\nu = 0.82$, under the initial conditions $(x(0),y(0),z(0)) = (0.1,0.2,0.25)$. Figure 14 shows the time evolution of the controlled states of the system (31). As we can see, the states $x(n)$, $y(n)$, and $z(n)$ converge towards zero asymptotically. This shows the accuracy and feasibility of the constructed control scheme.

7 Data analysis, results and discussion

We conclude our analysis using time-series plots in order to obtain a better comprehension of the proposed fractional-order biological model. For the parameter values mentioned in Table 1, Figure 15(a) and Figure 16(a) show the time evolution of cancer cells (C), healthy CD4+T lymphocyte cells (S), and

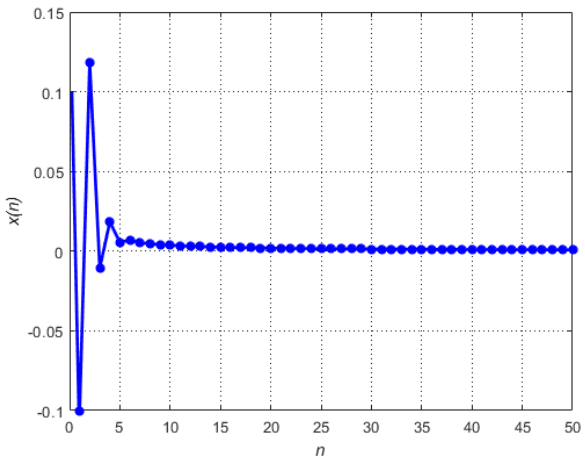

(a) $x(n)$ with n

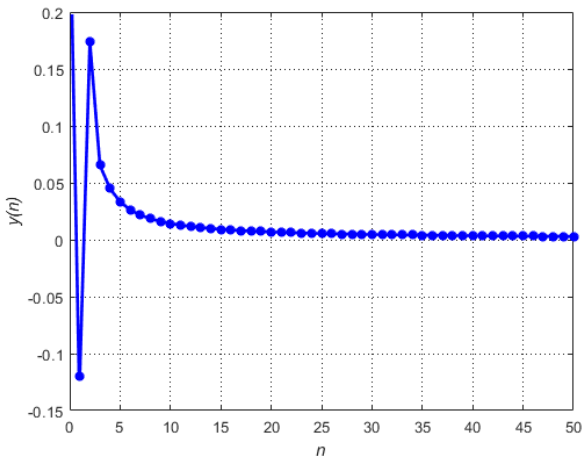

(b) $y(n)$ with n

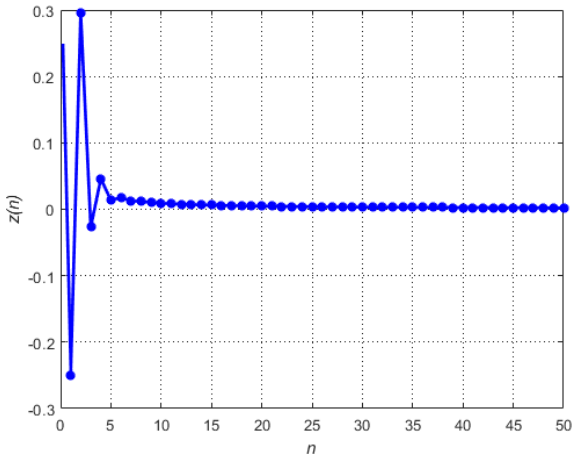

(c) $z(n)$ with n

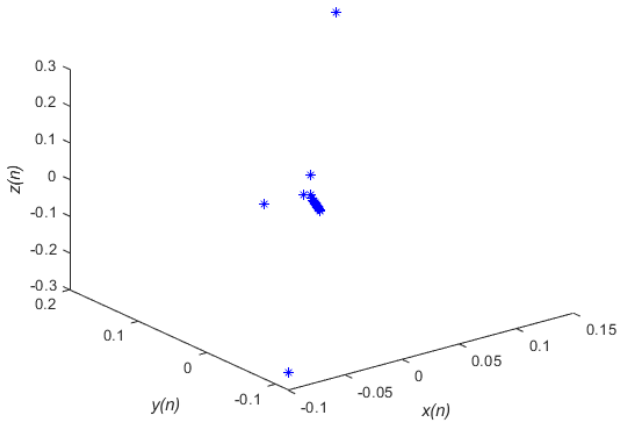

(d) phase space

Figure 14. Evolution of the controlled states of the commensurate fractional-order system (31) for $\nu = 0.82$

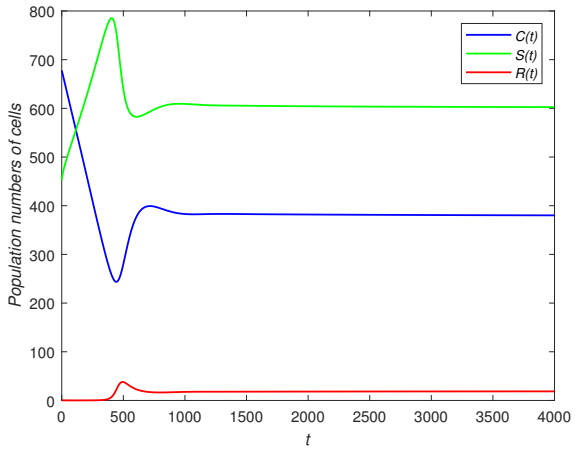

(a) Continuous F-O model for $\nu_1 = \nu_2 = \nu_3 = 0.69$

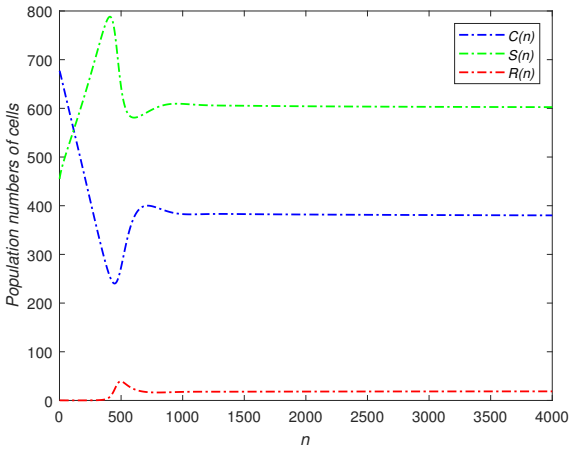

(b) Discrete F-O model for $\nu_1 = \nu_2 = \nu_3 = 0.69$

Figure 15. Time series of the fractional-order (F-O) models

Table 3. The minimum and maximum numbers of biological cells in the commensurate case $\nu_1 = \nu_2 = \nu_3 = 0.69$

Biological cells	Continuous fractional-order model (min,max)	Discrete fractional-order model (min,max)	Average number of biological cells
Cancer cells C	$(245, 678)$	$(240, 678)$	380
Healthy cells S	$(452, 784)$	$(452, 787)$	602
HIV-Infected Cells R	$(0, 37)$	$(0, 38)$	18

HIV-infected cells (R) of the continuous fractional-order model (10) for $\nu_1 = \nu_2 = \nu_3 = 0.69$ (commensurate fractional-order) and $(\nu_1, \nu_2, \nu_3) = (0.91, 0.92, 0.93)$ (non-commensurate fractional-order), respectively, while the time series plots obtained from the corresponding discrete fractional-order system constructed using the Caputo-like delta difference operator are shown in Figure 15(b) and Figure 16(b), respectively. By comparing the findings, we find that the results obtained from the continuous fractional-order system are identical to the results of the discrete fractional system. Using the time series results, we expect the population numbers of the three biological cells in sufficient time when the oscillations are stabilized for commensurate and non-commensurate fractional orders. The results are shown in Table 3 and Table 4. The average number of cell populations can help biologists collect statistical data to fight the disease.

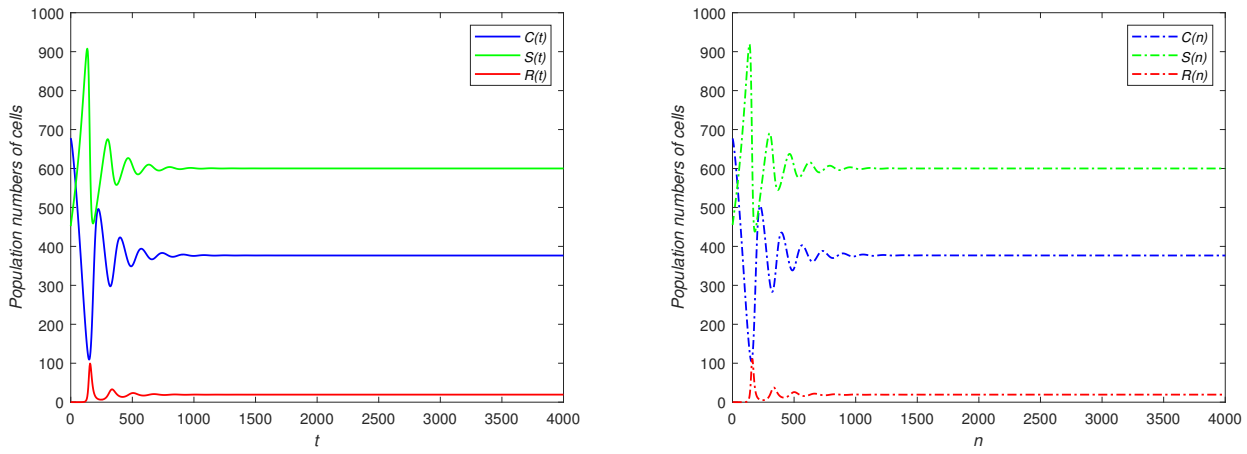

(a) Continuous model for $(\nu_1, \nu_2, \nu_3) = (0.91, 0.92, 0.93)$ (b) Discrete model for $(\nu_1, \nu_2, \nu_3) = (0.91, 0.92, 0.93)$

Figure 16. Time series of the fractional-order models

Table 4. The numbers of biological cells in the non-commensurate case $(\nu_1, \nu_2, \nu_3) = (0.91, 0.92, 0.93)$

Biological cells	Continuous fractional-order model (min,max)	Discrete fractional-order model (min,max)	Average number of biological cells
Cancer cells C	$(111, 678)$	$(114, 678)$	376
Healthy cells S	$(452, 907)$	$(452, 918)$	602
HIV-Infected Cells R	$(0, 99)$	$(0, 110)$	19

8 Conclusion

In this paper, a 3-D discrete-time fractional-order chaotic system which is composed of cancer, healthy, and HIV-infected cells is analyzed. We demonstrated that the biological system can exhibit chaotic behavior

for some parameter values. The dynamical behaviors are analyzed using powerful nonlinear dynamic analysis tools such as phase plots, bifurcation diagrams, and the maximum Lyapunov exponent, which show that the discrete system constructed using the Caputo-like-delta difference operator has rich dynamic behaviors. Furthermore, an efficient fractional-order controller is designed to stabilize the chaotic motions of the discrete system states. In biological systems, chaos and bifurcation are common phenomena. The biological implications of chaos and bifurcation in such a model involve studying population dynamics, where bifurcation points represent critical transitions. When the parameters change, the system can shift from a stable state to a chaotic state. Moreover, the chaotic dynamics can lead to population fluctuations, and then the extinction risk increases. Stable equilibria in a dynamical system are essential for species persistence, and bifurcation can lead to unstable fixed points. Thus, the transition to a chaotic state can lead to complex and unpredictable behavior. Understanding bifurcation behavior allows us to suggest efficient strategies to control chaotic dynamics in biological systems for the reasons stated above. Furthermore, researchers and biologists can use these insights to explain many biologically observed HIV-cancer states, including stable, periodic, quasiperiodic, and chaotic behaviors. Then, they can develop control techniques for suppressing chaos in biological dynamical systems.
In the near future, we plan to work on this topic, since we believe that controlling or suppressing chaos in fractional-order HIV-1 models involving AIDS-related cancer cells can help biologists and scientists in the fight against AIDS and cancer.

Declarations

Use of AI tools

he authors declare that they have not used Artificial Intelligence (AI) tools in the creation of this article.

Data availability statement

There are no external data associated with this article.

Ethical approval (optional)

The authors state that this research complies with ethical standards. This research does not involve either human participants or animals.

Consent for publication

Not applicable

Conflicts of interest

The authors declare that they have no conflict of interest.

Funding

No funding was received for this research.

Author's contributions

H.N.: Conceptualization, Methodology, Writing-Original draft preparation, Software. H.T.: Data Curation, Methodology, Supervision, Writing-original draft preparation, Validation. All authors have read and agreed to the published version of the manuscript.

Acknowledgements

The authors like to express their gratitude to everyone who helped to complete this research work.

References

[1] Daley, D.J. and Gani, J.M. *Epidemic Modelling: An Introduction*. Cambridge University Press: New York, (1999).

[2] Duarte, J., Januário, C., Martins, N., Ramos, C.C., Rodrigues, C. and Sardanyés, J. Optimal homotopy analysis of a chaotic HIV-1 model incorporating AIDS-related cancer cells. *Numerical Algorithms*, 77, 261–88, (2018). [CrossRef]

[3] Boshoff, C. and Weiss, R. AIDS-related malignancies. *Nature Reviews Cancer*, 2, 373–382, (2002). [CrossRef]

[4] Callaway, D.S. and Perelson, A.S. HIV-1 infection and low steady state viral loads. *Bulletin of Mathematical Biology*, 64(1), 29–64, (2002). [CrossRef]

[5] Naik, P.A., Yeolekar, B.M., Qureshi, S., Yeolekar, M. and Madzvamuse, A. Modeling and analysis of the fractional-order epidemic model to investigate mutual influence in HIV/HCV co-infection. *Nonlinear Dynamics*, 112, 11679–11710, (2024). [CrossRef]

[6] Saeed, T., Djeddi, K., Guirao, J.L., Alsulami, H.H. and Alhodaly, M.S. A discrete dynamics approach to a tumor system. *Mathematics*, 10(10), 1774, (2022). [CrossRef]

[7] Rogosin, S. and Dubatovskaya, M. Fractional calculus in Russia at the end of XIX century. *Mathematics*, 9(15), 1736, (2021). [CrossRef]

[8] Miller, K.S. and Ross, B. *An Introduction to the Fractional Calculus and Fractional Differential Equations*. Wiley-Interscience: New York, (1993).

[9] Samko, S.G., Kilbas, A.A. and Marichev, O.I. *Fractional Integrals and Derivatives: Theory and Applications*. Gordon and Breach Science Publishers: Philadelphia, USA, (1993).

[10] Kilbas, A.A., Srivastava, H.M. and Trujillo, J.J. *Theory and Applications of Fractional Differential Equations* (Vol. 204). Elsevier: Tokyo, (2006).

[11] Caputo, M. and Fabrizio, M. A new definition of fractional derivative without singular kernel. *Progress in Fractional Differentiation and Applications*, 1(2), 73-85, (2015). [CrossRef]

[12] Atangana, A. and Baleanu, D. New fractional derivatives with nonlocal and non-singular kernel: theory and application to heat transfer model. *Thermal Science*, 20(2), 763-769, (2016). [CrossRef]

[13] Debbouche, N., Ouannas, A., Grassi, G., Al-Hussein, A.B.A., Tahir, F.R., Saad, K.M. and Aly, A.A. Chaos in cancer tumor growth model with commensurate and incommensurate fractional-order derivatives. *Computational and Mathematical Methods in Medicine*, 2022, 5227503, (2022). [CrossRef]

[14] Chamgoué, A.C., Ngueuteu, G.S.M., Yamapi, R. and Woafo, P. Memory effect in a self-sustained birhythmic biological system. *Chaos, Solitons & Fractals*, 109, 160-169, (2018). [CrossRef]

[15] Gholami, M., Ghaziani, R.K. and Eskandari, Z. Three-dimensional fractional system with the stability condition and chaos control. *Mathematical Modelling and Numerical Simulation with Applications*, 2(1), 41-47, (2022). [CrossRef]

[16] Naik, P.A., Yavuz, M., Qureshi, S., Zu, J. and Townley, S. Modeling and analysis of COVID-19 epidemics with treatment in fractional derivatives using real data from Pakistan. *The European Physical Journal Plus*, 135, 795, (2020). [CrossRef]

[17] Naik, P.A. Global dynamics of a fractional-order SIR epidemic model with memory. *International Journal of Biomathematics*, 13(08), 2050071, (2020). [CrossRef]

[18] Yapışkan, D. and Eroğlu, B.B.İ. Fractional-order brucellosis transmission model between interspecies with a saturated incidence rate. *Bulletin of Biomathematics*, 2(1), 114-132, (2024). [CrossRef]

[19] Atede, A.O., Omame, A. and Inyama, S.C. A fractional order vaccination model for COVID-19 incorporating environmental transmission: a case study using Nigerian data. *Bulletin of Biomathematics*, 1(1), 78-110, (2023). [CrossRef]

[20] Omame, A., Onyenegecha, I.P., Raezah, A.A. and Rihan, F.A. Co-dynamics of COVID-19 and viral

hepatitis B using a mathematical model of non-integer order: impact of vaccination. *Fractal and Fractional*, 7(7), 544, (2023). [CrossRef]

[21] Nwajeri, U.K., Omame, A. and Onyenegecha, C.P. Analysis of a fractional order model for HPV and CT co-infection. *Results in Physics*, 28, 104643, (2021). [CrossRef]

[22] Omame, A. and Zaman, F.D. Analytic solution of a fractional order mathematical model for tumour with polyclonality and cell mutation. *Partial Differential Equations in Applied Mathematics*, 8, 100545, (2023). [CrossRef]

[23] Munir, S., Omame, A. and Zaman, F.D. Mathematical analysis of a time-fractional coupled tumour model using Laplace and finite Fourier transforms. *Physica Scripta*, 99(2), 025241, (2024). [CrossRef]

[24] Holm, M. *The Theory of Discrete Fractional Calculus: Development and Application*. Ph.D. Thesis, Department of Mathematics, The University of Nebraska-Lincoln, (2011). [https://digitalcommons.unl.edu/mathstudent/27/]

[25] Podlubny, I. *Fractional Differential Equations* (Vol. 198). Academic Press: San Diego, (1999).

[26] Diaz, J.B. and Osler, T.J. Differences of fractional order. *Mathematics of Computation*, 28(125), 185-202, (1974). [CrossRef]

[27] Atici, F.M. and Eloe, P. Discrete fractional calculus with the nabla operator. *Electronic Journal of Qualitative Theory of Differential Equations*, 3, 1-12, (2009). [CrossRef]

[28] Abdeljawad, T. On Riemann and Caputo fractional differences. *Computers & Mathematics with Applications*, 62(3), 1602-1611, (2011). [CrossRef]

[29] Abdeljawad, T., Baleanu, D., Jarad, F. and Agarwal, R.P. Fractional sums and differences with binomial coefficients. *Discrete Dynamics in Nature and Society*, 2013, 104173, (2013). [CrossRef]

[30] Andreichenko, K.P., Smarun, A.B. and Andreichenko, D.K. Dynamical modelling of linear discrete-continuous systems. *Journal of Applied Mathematics and Mechanics*, 64(2), 177-188, (2000). [CrossRef]

[31] Goodrich, C. and Peterson, A.C. *Discrete Fractional Calculus*. Springer Cham: Switzerland, (2015). [CrossRef]

[32] Devaney, R. *An Introduction to Chaotic Dynamical Systems*. CRC Press: USA, (2003). [CrossRef]

[33] Strogatz, S.H. *Nonlinear Dynamics and Chaos With Applications to Physics, Biology, Chemistry, and Engineering*. CRC Press: USA, (2018). [CrossRef]

[34] Anastassiou, G.A. Principles of delta fractional calculus on time scales and inequalities. *Mathematical and Computer Modelling*, 52(3-4), 556-566, (2010). [CrossRef]

[35] Cermák, J., Gyori, I. and Nechvátal, L. On explicit stability conditions for a linear fractional difference system. *Fractional Calculus and Applied Analysis*, 18, 651-672, (2015). [CrossRef]

[36] Lou, J., Ruggeri, T. and Tebaldi, C. Modeling cancer in HIV-1 infected individuals: equilibria, cycles and chaotic behavior. *Mathematical Biosciences and Engineering*, 3(2), 313-324, (2006). [CrossRef]

[37] Naik, P.A., Owolabi, K.M., Yavuz, M. and Zu, J. Chaotic dynamics of a fractional order HIV-1 model involving AIDS-related cancer cells. *Chaos, Solitons & Fractals*, 140, 110272, (2020). [CrossRef]

[38] Cafagna, D. and Grassi, G. Fractional-order systems without equilibria: the first example of hyperchaos and its application to synchronization. *Chinese Physics B*, 24(8), 080502, (2015). [CrossRef]

[39] Wu, G.C. and Baleanu, D. Jacobian matrix algorithm for Lyapunov exponents of the discrete fractional maps. *Communications in Nonlinear Science and Numerical Simulation*, 22(1-3), 95-100, (2015). [CrossRef]

[40] Sun, K.H., Liu, X. and Zhu, C.X. The 0-1 test algorithm for chaos and its applications. *Chinese Physics B*, 19(11), 110510, (2010). [CrossRef]

[41] En-Hua, S., Zhi-Jie, C. and Fan-Ji, G. Mathematical foundation of a new complexity measure. *Applied Mathematics and Mechanics*, 26, 1188-1196, (2005). [CrossRef]

[42] Pincus, S.M. Approximate entropy as a measure of system complexity. *Proceedings of the National Academy of Sciences*, 88(6), 2297-2301, (1991). [CrossRef]

Mathematical Modelling and Numerical Simulation with Applications (MMNSA)
(https://dergipark.org.tr/en/pub/mmnsa)

How to cite this article: Nabil, H. & Tayeb, H. (2024). A three-dimensional discrete fractional-order HIV-1 model related to cancer cells, dynamical analysis and chaos control. *Mathematical Modelling and Numerical Simulation with Applications*, 4(3), 256-279. https://doi.org/10.53391/mmnsa.1484994